USE OF PIEZOELECTRIC AND FERROELECTRIC MATERIALS IN ULTRASONIC TRANSDUCERS

W. Mason

USE OF PIEZOELECTRIC AND FERROELECTRIC MATERIALS IN ULTRASONIC TRANSDUCERS

W. P. MASON

Columbia University, New York NY 10027, U. S. A.

Résumé. — Après un rappel des travaux initiaux de Langevin sur l'utilisation du quartz, l'étude porte sur les matériaux qui ont été ensuite utilisés à cet effet.

Après la magnétostriction, sont étudiées en détail les propriétés de cristaux piézoélectriques : le sel de Rochelle et l'ADP (phosphate d'ammonium). Les points de Curie, les coefficients de couplage et les circuits équivalents sont fournis. Dans le cas de l'ADP, plusieurs kilowatts d'énergie acoustique ont pu être obtenus en impulsions d'environ 10^{-4} s.

L'étude aborde ensuite l'utilisation des matériaux ferroélectriques et tout d'abord du titanate de baryum. Les conditions d'obtention de monocristaux ou de céramiques sont décrites. Les coefficients piézoélectriques, les constantes diélectriques et les coefficients de dilatation sont étudiés en fonction de la température. L'expression thermodynamique de l'énergie libre est donnée. Les qualités et limitations de ce matériau comme transducteur sont étudiées.

Etude analogue des solutions solides de titanate et de zirconate de plomb. Le diagramme de phase est donné, montrant le rôle critique de la concentration de 52 % du $PbTiO_3$. Le rôle de certaines impuretés est étudié.

Il est possible, grâce à un dispositif décrit, d'utiliser ces céramiques dans le domaine de fréquence des kilohertz. Dans le fonctionnement en impulsion, des puissances de l'ordre du mégawatt ont été atteintes.

Pour produire des fréquences très élevées (au-dessus de 100 MHz), on utilise des monocristaux ferroélectriques de niobate et de tantalate de lithium ou de niobate de baryum et de sodium ($Ba_2NaNb_3O_{15}$).

Finalement pour les fréquences supérieures à 500 MHz, il convient de recourir aux films obtenus par évaporation ou par pulvérisation cathodique (oxyde de zinc et sulfure de cadmium).

Abstract. — After recalling Langevin's first works with quartz transducers, this paper describes transducer materials which have been developed later.

The piezoelectric parameters, such as Curie temperature, or electromechanical coupling factor of Rochelle salt and ADP (ammonium dihydrogen phosphate) are exposed. Using ADP, many kilowatts of acoustic energy have been obtained in 10^{-4} s duration pulses.

Ferroelectric materials are described, starting with barium titanate. The preparation of the material is described. Piezoelectric, dielectric and expansion constants are studied as a function of temperature leading to the limitations of such a material for transducer work.

A similar description is given for lead titanate-lead zirconate solid solutions. The phase diagram shows the existence of a critical concentration of $PbTiO_3$. The influence of some impurities is investigated.

Using such ceramic transducers operating in pulses peak power of megawatts can be obtained in pulsed work.

For very high frequencies (above 100 MHz) single crystals of lithium niobate or lithium tantalate can be used. Barium sodium niobate has been used as a non-linear crystal.

Finally, operation above 500 MHz requires evaporated or sputtered thin film transducers.

1. **Introduction.** — Since this is the 100th anniversary of the birth of Prof. Paul Langevin, it is proper that an account be given of the field of ultrasonics. This follows since Langevin was the first one to produce an underwater sound transducer for measuring depths and for locating submarines. His depth sounding transducer is shown by figure 1. In this transducer thin plates of quartz are cemented between steel plates which were used to bring the frequency of the transducer down to 50 kHz. This device was not developed until after the war but was successful in measuring depths and in locating submarines. It was the prototype of all subsequent underwater sound transducers.

Crystalline quartz has many drawbacks when used as an underwater sound material. Some of these are high electrical impedance, low electromechanical coupling coefficient, and relatively high price. At the present time quartz is used only to generate very high frequency shear and longitudinal waves for measurement purposes and in very selective crystal filters (coil and condenser [1] and monolithic types [2]). Here the very high Q and the very low temperature coefficient obtainable in various crystal

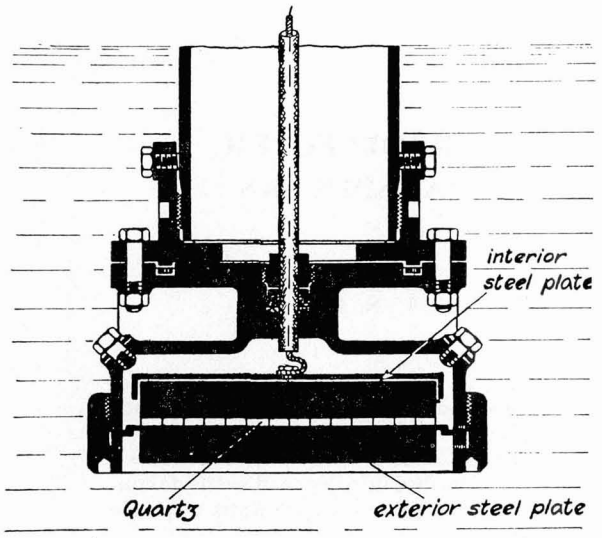

FIG. 1. — Langevins apparatus for depth sounding.

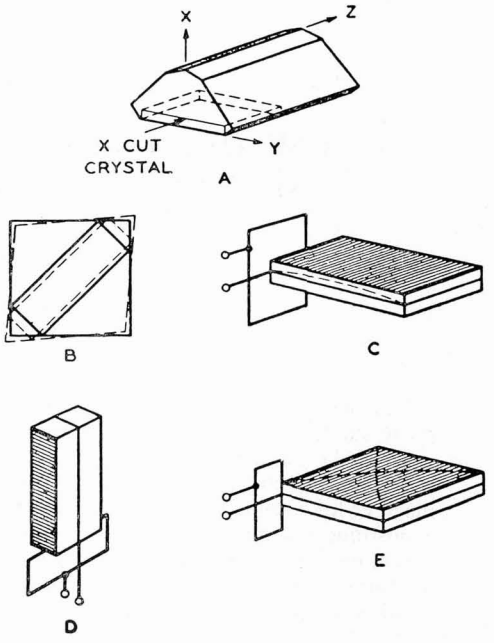

FIG. 2. — Rochelle salt crystals and principal cuts.

cuts [3] more than outweigh the low coupling coefficients. Such filters are used as selecting elements in all the carrier current, microwave, and underwater cable communication systems of the Bell Telephone company.

2. **Transducer crystals after quartz.** — Since this colloquium is partly historical, it is worth considering the successors to quartz as electromechanical driving elements. Nickel magnetostrictive tubes were rather widely used in the United States and this and other metals have been the principal transducer materials in Japan [4], [5]. On account of eddy currents which cut down the efficiency and the limiting stress that can be obtained before saturation occurs, piezoelectric crystals were also used in the United States.

The first crystal employed by the US Navy was Rochelle salt. This grows in the orthorhombic form shown by figure 2. Rochelle salt is a ferroelectric crystal with the X direction being the ferroelectric axis along which spontaneous polarization occurs. The crystal cut of interest in underwater sound transducers is the 45 degrees X cut shown by figure 2*b*. When a voltage is applied along the X axis the crystal elongates. Since the backing plate on which the crystals are mounted has a much higher mechanical impedance than the crystals, they will resonate as quarter wave devices. The arrangement of four crystals per unit block on the inside and two on the outside — as shown by figure 3 — produces the directional pattern shown by the bottom left part of the figure. The whole transducer was mounted in a case filled with castor oil and the acoustic energy was transmitted to the sea water through a rubber face plate.

The properties of Rochelle salt vary a considerable amount with temperature but in the range for which an underwater transducer is used, i. e. 0° to 24 °C, the principal property, the electromechanical coupling factor, varies only from 0.6 to 0.88 as shown by figure 4. This factor, which is defined as the square root of the ratio of the electrical (mechanical) work which can be done under ideal conditions, to the total energy stored from a mechanical (electrical) source. This coupling factor determines the frequency band over which most of the electrical energy can be transformed into mechanical energy or vice versa. This follows from the equivalent circuit for a quarter wave crystal — shown by figure 5*a* — which was first derived by the writer [6]. The element values are given in terms of the piezoelectric constant d_{12}, the elastic compliance constant s^E_{22} (the superscript E indicates that the elastic compliance is measured at constant field), the dielectric constant ε^T_{11} (measured at constant stress), the density ρ, and the dimensions of the crystal. Since the equivalent circuit is in the form of a band pass filter, the region of good transmission can be derived from the filter formula. However a much wider frequency range can be obtained by resonating the shunt capacitance C_0 by means of the electrical coil L_0 as shown by figure 5*b*. For this combination the filter parameters are given by eq. (1)

$$
\begin{aligned}
C_1 \psi^2 &= \frac{8}{\pi^2} \frac{lw}{t} \frac{d_{12}^2}{s_{22}^E} = \frac{f_2 - f_1}{2 \pi f_1 f_2 Z_0}; \\
C_0 &= \frac{\varepsilon^S lw}{t} = \frac{1}{2 \pi (f_2 - f_1) Z_0}; \\
L_0 &= \frac{(f_2 - f_1) Z_0}{2 \pi f_1 f_2}; \\
\frac{M_1}{\varphi^2} &= \frac{\rho l t}{2 w} \left(\frac{s_{22}^E}{d_{12}} \right)^2 = \frac{Z_0}{2 \pi (f_2 - f_1)};
\end{aligned}
\qquad (1)
$$

where Z is the mid shunt characteristic impedance.

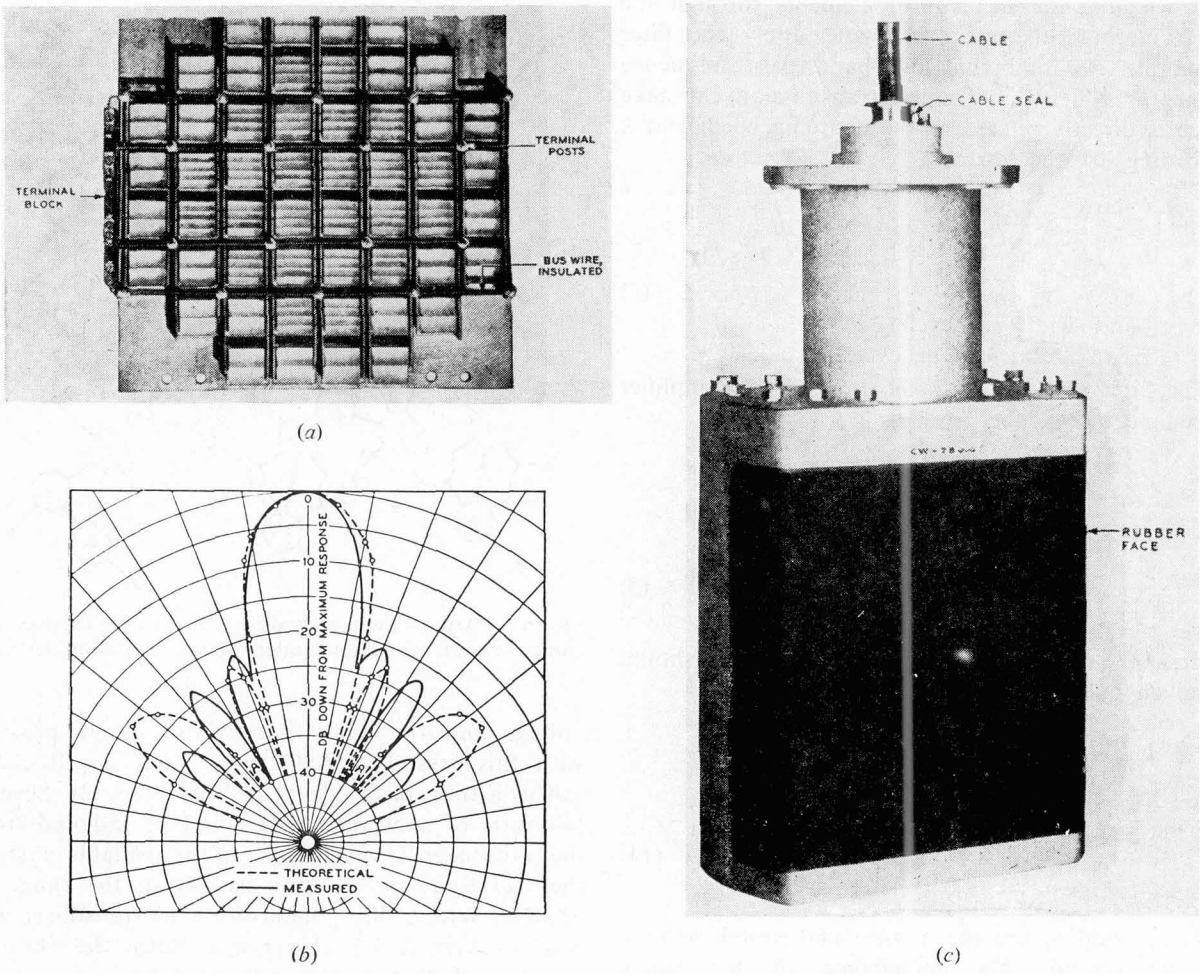

FIG. 3. — Use of Rochelle salt and ADP crystals as underwater sound transducers. Top left : crystal array for QJA underwater sound transducer. Bottom left : Theoretical and measured directional pattern of QJA transducer. Right : Case and *pc* rubber transparent window for QJA transducer.

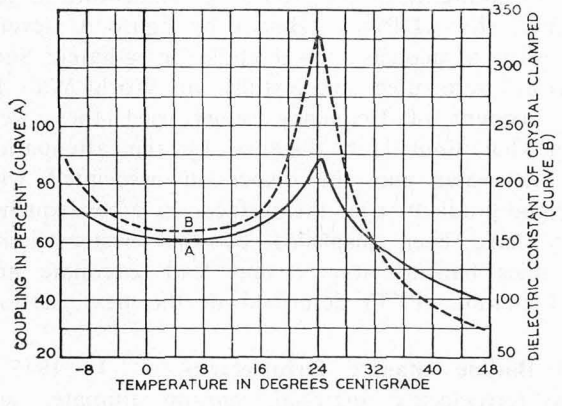

FIG. 4. — Curve *A* represents the electromechanical coupling constant of a Rochelle salt crystal. Curve *B* represents the dielectric constant of the crystal clamped.

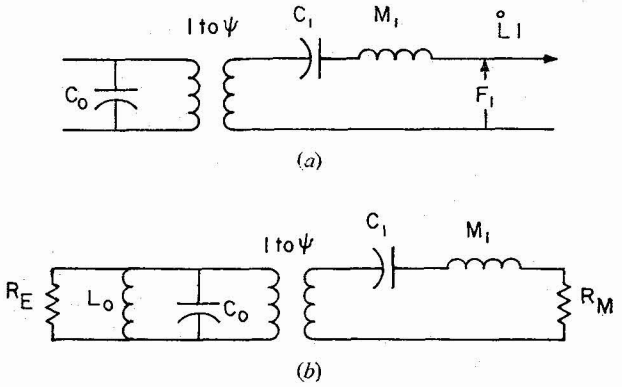

FIG. 5. — A. Equivalent circuit of a Quarter Wave piezoelectric transducer. B. Filter circuit for determining pass band of a transducer.

a) $C_0 = \frac{\varepsilon^s lw}{t}$; $C_1 = \frac{8}{\pi^2}\frac{lw}{t}s_{22}^E$; $M_1 = \frac{\rho lwt}{2}$; $\psi = \frac{d_{12}\,w}{s_{22}^E}$.

b) $\frac{f_2 - f_1}{f_M} = \frac{BW}{f_M} = \sqrt{\frac{8}{\pi^2}}\frac{k}{\sqrt{1-k^2}}$.

If we take the mechanical elements through the electromechanical transformer and apply the filter equations, we find that the band pass frequency range for which good sound transmission can take place is directly related to the coupling coefficient k according to the formula

$$\frac{f_2 - f_1}{f_M} = \frac{BW}{f_M} = \sqrt{\frac{8}{\pi^2}} \sqrt{\frac{d_{12}^2}{\varepsilon^S s_{22}^E}} = \sqrt{\frac{8}{\pi^2}} \frac{k}{\sqrt{1 - k^2}}; \tag{2}$$

BW = band width in cycles,
f_M = mean frequency in cycles.

The filter parameters show also that the amplifier impedance should be given by eq. (3)

$$Z_0 = R_E = \sqrt{\frac{\pi^2}{8}} \frac{\sqrt{1 - k^2}}{k} \sqrt{\frac{L_0}{C_0}}$$

$$= \sqrt{\frac{\pi^2}{8}} \frac{\sqrt{1 - k^2}}{k} \left[\frac{t}{2 \pi f_M \varepsilon^S lw}\right] \tag{3}$$

whereas the mechanical impedance termination should be given by eq. (4),

$$R_M = Z_0 \psi^2 = \frac{1}{\sqrt{2}} \frac{k}{\sqrt{1 - k^2}} \sqrt{\frac{\rho}{s_{22}^E}} wt$$

$$= \frac{1}{\sqrt{2}} \frac{k}{\sqrt{1 - k^2}} (\rho v)_c \, wt \tag{4}$$

where ρ_c and v_c are the density and sound velocity of the crystal. The impedance of sea water $Z = \rho v = 1.5 \times 10^5$ mechanical ohms per square cent is close enough to produce a reasonable match for this condition for Rochelle salt with $\rho v = 7 \times 10^5$. If $k = 0.6$ then $R_M = 4 \times 10^5$ mechanical ohms. Lower coupled crystals such as ADP give a better match.

In 1935 a new series of water soluable crystals was discovered by Busch and Scherrer in Zurich. Of these the most interesting one for transducer applications was ammonium dihydrogen phosphate which received the abbreviation ADP. The crystal is stable from — 125 °C — below which a transition occurs which pulverizes the crystal — up to 100 °C. This transition is associated with a lining up of the dielectric dipoles along one line [8], as shown by figure 6, and a reversal of the dipoles along adjacent lines, an antiferroelectric condition. ADP was the first antiferroelectric crystal discovered. The change in the direction of polarization is associated with considerable strain and this results in the crystal fracture. Since this occurs at a very low temperature it does not interfere with the crystal as a transducer. In the room temperature range the coupling coefficient is 30 % and hence from eq. (2) the bandwidth of the transducer is also about 30 %. The arrangement of the crystals on the backing plate is the same as that shown on figure 3. The higher breakdown

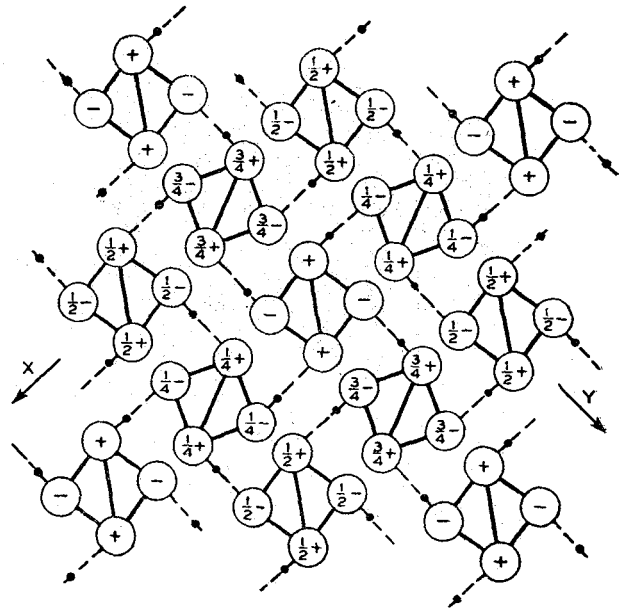

FIG. 6. — Arrangement of hydrogen neuclei to produce and antiferroelectric condition (after Mason and Matthias [8]).

voltage and the wider temperature range possible with this crystal caused them to replace Rochelle salt as a transducer crystal in World War II. Several kilowatts of acoustic power could be radiated from the transducer. Due to the size of the available crystals, the mid frequency f_M was usually in the range of 25 kHz. With a 30 % bandwidth the transducer was efficient over a 7.5 kHz range. Since the shortest pulse length that can be radiated from such a transducer is given by the equation

$$\Delta t = \frac{1.4}{BW} \doteq 1.86 \times 10^{-4} \text{ s} \tag{5}$$

for this ADP transducer. This allows one to separate out pulses from distances of 28 feet or farther. For depth sounders working to 2 to 3 feet, the frequency has to be higher or the percentage bandwidth larger.

With the ADP unit shown by figure 3, several kilowatts of acoustic power could be radiated. Such devices were used successfully in World War II. On account of frequency range used they were somewhat limited in distance by the attenuation of sea water and the dispersion associated with thermal gradients near the surface. As a consequence they have been displaced by the electrostrictive ceramics barium titanate and lead zirconate and lead titanite (PZT) described in the next section.

3. **Barium titanate ferroelectrics.** — In 1945 a new ferroelectric material, barium titanate, was discovered and this and similar structures have turned out to be the most useful and interesting ferroelectrics. Barium titanate was discovered at about the same time by Von Hippel, Breckenridge, Chesley and Tisza at MIT [9] and by Vul and Gold-

man [10] in Russia. It can be produced in ceramic form and be given its ferroelectric properties by a polarization process. Figure 7 shows a measurement

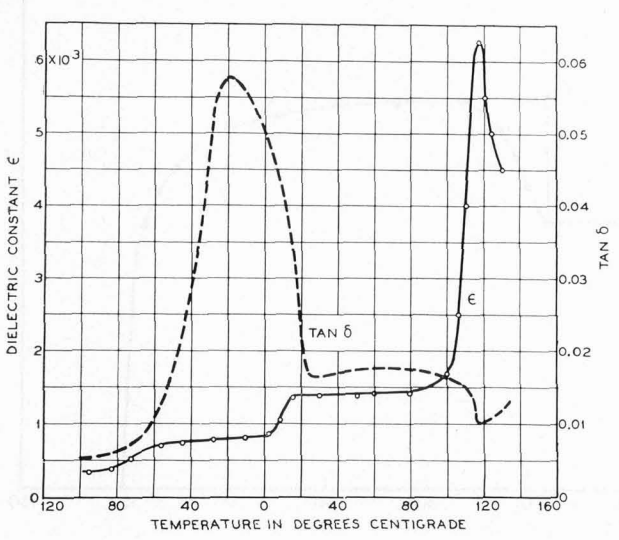

FIG. 7. — Dielectric constant and dissipative function for an unpolarized barium titanate ceramic (after Von Hippel *et al.* [9]).

of the dielectric constant and the dissipative function tan δ for an unpolarized ceramic over a large temperature range. It is obvious that there are three temperatures for which a transition occurs from one dielectric constant value to another, with a change also in the tan δ function.

Single crystals of barium titanate have been grown mostly by the Remeika [11] method. These allow a better determination of the properties than can be obtained from the ceramic. Figure 8 shows a measurement of the dielectric constant and the dissipative function

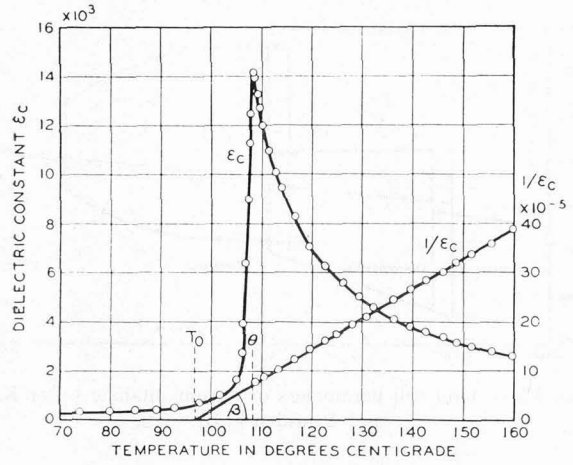

FIG. 8. — Dielectric constant along the c axis as a function of the temperature. $\varepsilon_c = A + B(T - T_0^P$ for $T > T^P$ (after Merz [12]).

surement of the dielectric constant along the ferroelectric axis made by Merz [12]. Above a critical temperature designated T_0^P, the dielectric constant follows the Curie-Weiss law that the inverse of the dielectric constant is propertional to the temperature. If we extrapolute to a zero value of $1/\varepsilon_0$ the temperature T_0 is about 10 °C lower than T_0^P. This difference is a measurement of the effect of the electromechanical coupling on the dielectric constant.

The next illustration, figure 9, is a measure of the dielectric constant along the c ferroelectric axis and

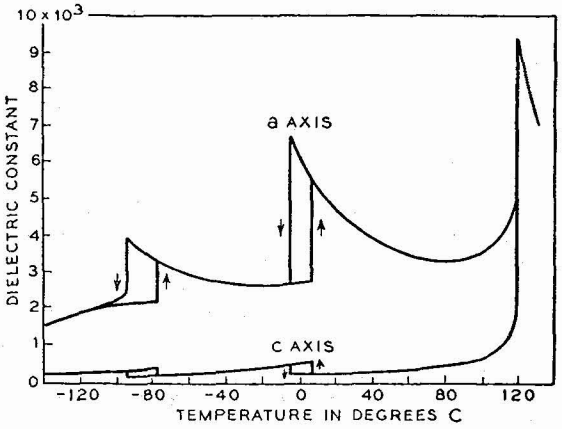

FIG. 9. — Complete measurements of dielectric constants along the a axis and c axis (after Merz [12]).

the a axis at right angles, as determined by Merz [12]. The three transition temperatures are obvious from the measurement. Merz also measured the spontaneous polarization, as shown by figure 10. It will be noted that the polarization along the c axis drops by $1/\sqrt{2}$ in the second region and $1/\sqrt{3}$ in the third region. It is also obvious that if the polarization in the highest region is reversed in a millionth of a second, which is possible, about 30 A/cm^2 are obtained by the process. Hence considerable electric energy can be obtained from a mechanical reversal or destruction of the polarization in a short time.

Figure 11 shows the hysteresis loop of a barium titanate crystal. With the square corners, one might expect that such a crystal could be used in information storage, as is common with ferromagnetic cores. However, it was found that after a number of reversals, the height of the loop declines and the corners become less square. Hence this use did not become practical.

Devonshire [13] first applied thermodynamics to the properties of barium titanate. Writing the free energy in the form of an expansion in even powers of the polarization along the three axes, as shown by eq. (6)

$$G_1 = 2\pi C^{-1}(T - T_0)(P_x^2 + P_y^2 + P_z^2) + \tfrac{1}{4} B v^3 g^4 \times (P_x^4 + P_y^4 + P_z^4) + \tfrac{1}{6} B' v^5 g^6 (P_x^6 + P_y^6 + P_z^6) + \tfrac{1}{2} B'' v^3 g^4 (P_x^2 P_y^2 + P_x^2 P_z^2 + P_y^2 P_z^2), \quad (6)$$

he showed that there was a possibility of four solu-

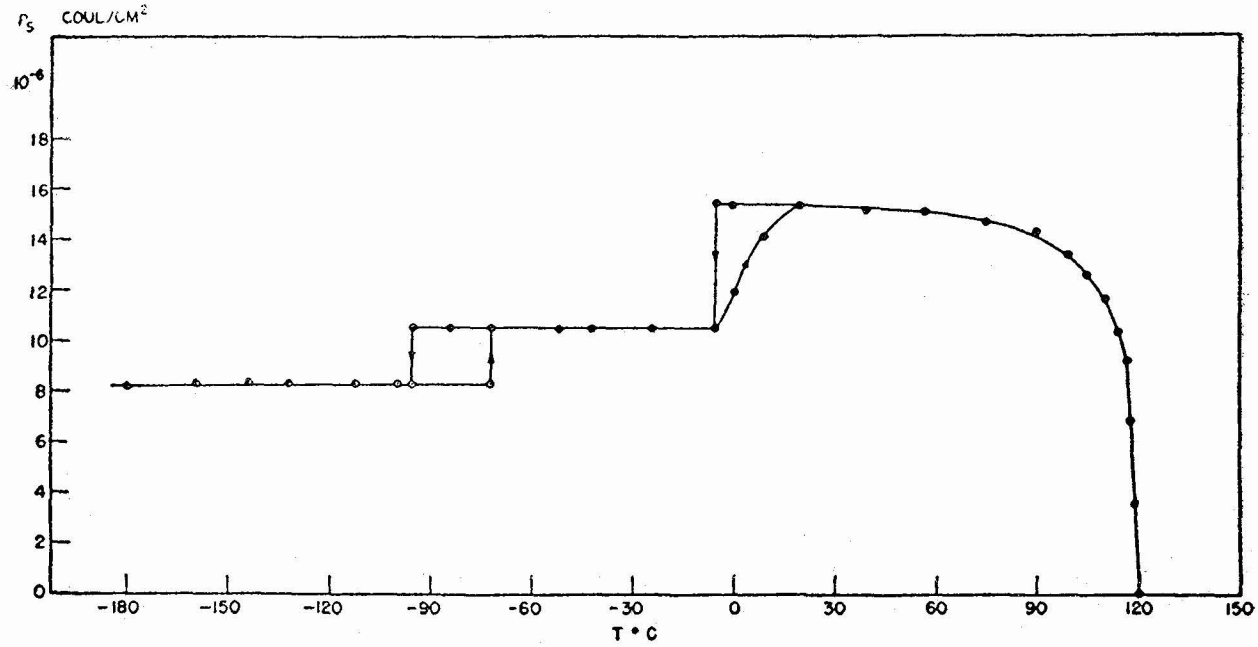

FIG. 10. — Spontaneous polarization along one axis over a temperature range (after Merz [12]).

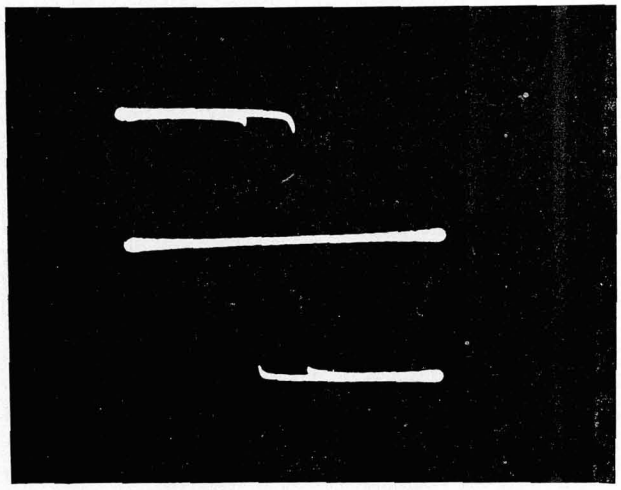

FIG. 11. — Hysteresis loop of a single crystal of barium titanate.

tions for the spontaneous polarizations along the three axes. The solutions obtained are

$$\begin{aligned} &P_x = P_y = P_z = 0\,, && \text{above Curie temperature}\,,\\ &P_x = P_y = 0\,;\, P_z \neq 0\,, && \text{at } 120\ ^\circ\text{C to } 10\ ^\circ\text{C}\,,\\ &P_x = 0\,;\, P_y = P_z \neq 0\,, && \text{at } -90\ ^\circ\text{C to } 10\ ^\circ\text{C}\,,\\ &P_x = P_y = P_z \neq 0\,, && \text{below } -90\ ^\circ\text{C}\,. \end{aligned} \qquad (7)$$

To agree with the polarizations observed in figure 10, the coefficient of the P^2 has to vanish at the Curie temperature and follow the form shown by the first term, where C is the Curie dielectric constant. The terms involving the fourth power have to be negative while the terms involving the sixth power of the polarization have to be positive. The values of the constants can be evaluated from the transition temperatures.

If one wishes to study the strains accompaning the phase changes, it is necessary to introduce terms in the free energy involving products of the strains times the squares and products of the polarizations. However, one can regard the distortion associated with the three phases as slight distortions of the cubic phase associated with the products of the square of the polarizations by the electrostrictive constants of which there are three for a cubic crystal. These constants can be evaluated by using the unit cell parameters determined by Kay and Vousden [14] and shown in figure 12 plotted as a function of the

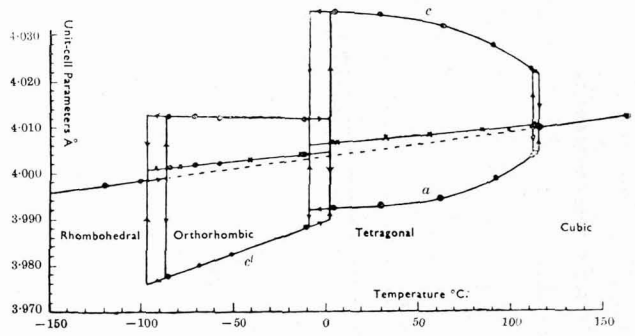

FIG. 12. — Unit cell parameters of barium titanate (after Kay and Vousden [14]).

temperature. In the cubic phase existing above 120 °C, all axes are equal. Below 120 °C, one axis — the ferroelectric axis — becomes 1 % larger than the other two. The two longitudinal constants can be evaluated in the tetragonal range from the expansions divided by the square of the polarization. The shear constant can be evaluated from the three unit cell dimensions

in the orthorhombic phase. Knowing these values, one can account for the changes in the unit cell dimensions for the three axes as shown by figure 13.

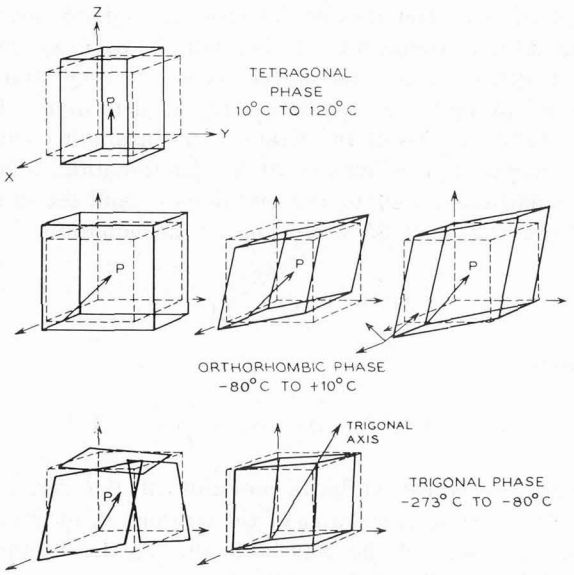

FIG. 13. — Electrostriction dimensional changes in barium titanate for the three phases.

For the tetragonal phase, the polarization is along a cube axis, and this results in an expansion along the polarization direction and a contraction along the other two. For the orthorhombic phase, the polarization is along a face diagonal. These results in an expansion of two of the axes, a contraction of the third, and a shearing strain in the plane of polarization. All of these strains are shown on the right-hand figure. To get an orthorhombic structure we have to take axes at 45 degrees to the cubic axes, in which case the unit cell will have three different values. Finally, when the polarization is along a cube diagonal, the spontaneous strains are all shearing modes. When these are added together, a trigonal phase results with the trigonal axis along a cube diagonal.

All the applications of barium titanate and related compounds involve the ceramic rather than the single crystal. On account of the high dielectric constants, small-sized condensors have been used in most television sets. However, the largest application is in connection with polarized ceramics used in electromechanical transducers. Figure 14 shows the modes of motion that can be generated in a polarized ceramic. By flipping over domains in the direction of the applied field and by squeezing domains at right angles to the applied field, the ceramic acquires a permanent polarization. If now an alternating field is superposed on this permanent polarization, it generates an expansion in the direction of the applied field, and a radial contraction at right angles to the field. A third mode of motion can be generated by polarizing in one direction and

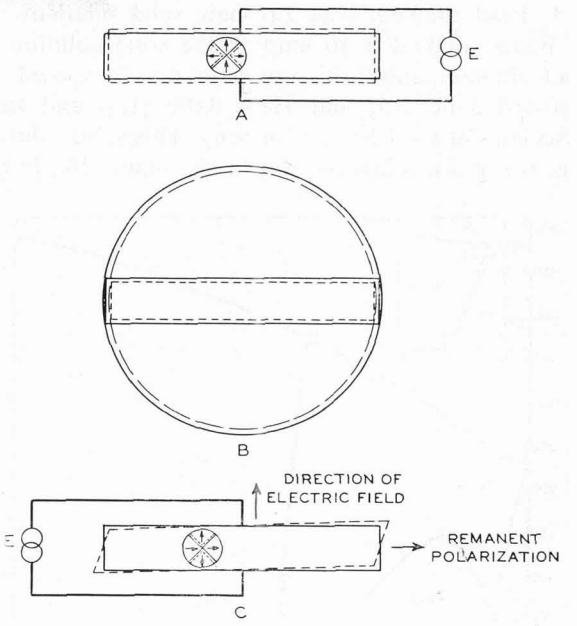

FIG. 14. — Modes of motion generated in a polarized ferroelectric ceramic.

applying a field in a perpendicular direction. This generates a thickness shear mode that has been used in sending shear waves in delay lines.

The constants of barium titanate are not too satisfactory, as shown by the data of figure 15. The

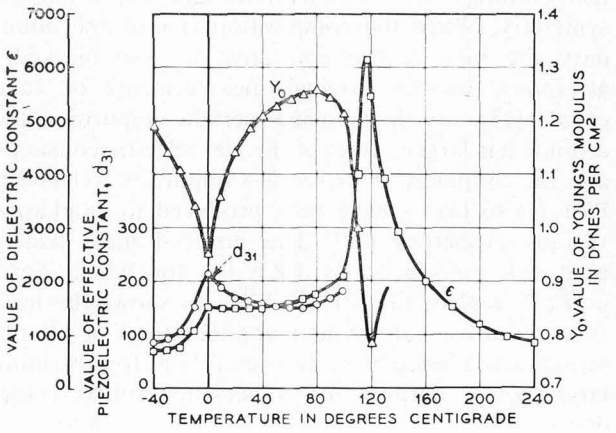

FIG. 15. — Dielectric constant, piezoelectric constant and Young's modulus for a polarized barium titanate ceramic.

Young's modulus shows big dips at the Curie temperature and at the tetragonal-orthorhombic transition temperature. The same is true for the dielectric constant and the piezoelectric constant d_{31} which determines the radial coupling constant $k_r = 0.36$. The thickness longitudinal mode has a value 0.50, while the face shear mode has a coupling of 0.48. One method for stabilizing the ceramic is to introduce a certain amount of calcium titanate or lead titanite, which lowers the second transition temperature and raises the Curie temperature. However, this occurs at the expense of the coupling coefficient.

4. **Lead titanate, lead zirconate solid solutions.** — A better method is to employ the solid solution of lead titanate and lead zirconate first proposed by Bernard Jaffe [15] and Hans Jaffe [16], and their associates at the Clevite Company. This solid solution has the phase diagram shown by figure 16. For a

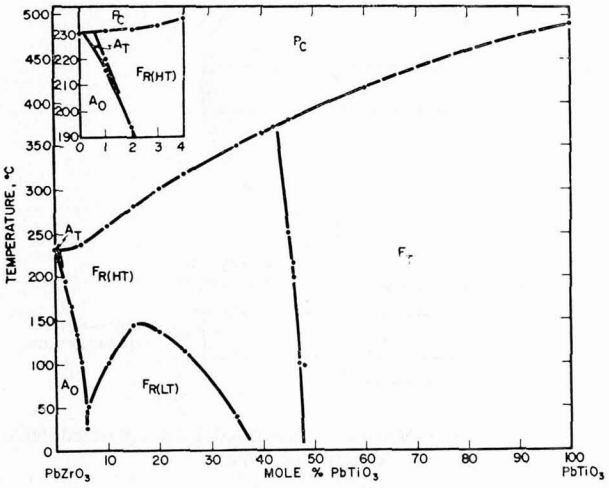

FIG. 16. — Lead zirconate-lead titanate phase diagram (after Berlincourt [17]).

solution having less than 52 % of lead titanate $PbTiO_3$, the combination has tetragonal symmetry while if the solution has more than 52 % at room temperature, the combination has orthorhombic symmetry. When the composition is near the boundary the piezoelectric constants increase markedly as shown by the original measurements of Jaffe *et al.* [15]. By introducing certain impurities the ceramic has larger values of the piezoelectric constants and the couplings. A series of 8 impurities — labelled PZT (1) to (8) — have been produced to emphasize various properties [17]. The material most widely used for transducers is PZT (8) for which Sc^{3+} or Fe^{3+} replace $(Ti, Zr)^{4+}$. PZT (8) shows the least effect of drive voltage and applied stress of all the ceramics and hence is the most useful one for obtaining large power outputs for underwater sound transducers.

In order to obtain low attenuations and freedom from thermal gradient effects these transducers have gone down in frequency in to the low kHz range. Figure 17 shows one method for producing low

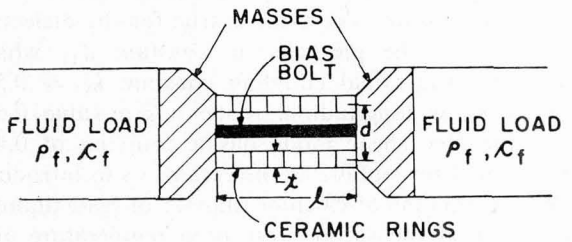

FIG. 17. — Low frequency ceramic transducer using axially polarized ceramic (after Berlincourt).

frequencies from ceramic materials [18]. A series of cylindrical disks, usually polarized along the axial direction, are cemented and held together by a bias bolt attached to two end masses. The length l and the two end masses are large enough to obtain the desired frequency. If this unit is used as part of a quarter wave transducer, as in the ADP transducer of figure 3, the frequency is determined by the total stiffness of the ceramic and bias bolt — and by neglecting the masses of the combination which is small compared to the end mass — and the value of the end mass M, according to the equation

$$f_R = 2\pi \sqrt{\frac{S_c + S_b}{M}} \qquad (8)$$

where

$$S_c = \frac{1}{l}(A_c \times c_{33}); \quad S_b = \frac{1}{l}(A_b \times Y_0).$$

Here c_{33} is the stiffness modulus of the ceramic, A_c the cross-sectional area of the ceramic, A_b the cross-sectional area of the bias bolt, and Y_0 the Young's modulus of the bolt material.

For continuous operation the limit to the power output is connected with the heating of the ceramic. Various conditions are discussed in reference [17]. However, for pulsing conditions, as in underwater sound transducers, heating is less important and it is usually the tensile strength that determines the limiting output. For the most used material PZT (8) this is about 7 000 pounds per square inch. By introducing the bias bolt shown, the limiting tensile strength can be increased and the power output raised. In order to obtain the necessary directivity at the low frequencies used, the area has to be large. With such transducers, the power output has been in the megawatt range.

Other methods for obtaining low frequencies are by the use of barrel staves vibrating in flexure. In order to obtain the necessary size, cemented joints are often used in the ceramic. These joints can be made as strong as the ceramic itself.

A potential application, which has so far not been reduced to practice, is in coupling a vibration engine to a ceramic flexure plate as shown by figure 18 [19]. According to calculations a considerable amount of electric power could be obtained for a very small weight unit.

5. **Single crystal ferroelectrics for ultra high frequency transducers.** — Ferroelectric ceramics are limited in frequency by the grain size of the material, by the internal dissipation — both electrical and mechanical —, and by the very low electrical impedance associated with the high dielectric constants. Frequencies above 100 mHz have become important for such applications as dispersive and non-dispersive delay lines, ultrasonic light deflectors and ultrasonic light modulation devices. These require high

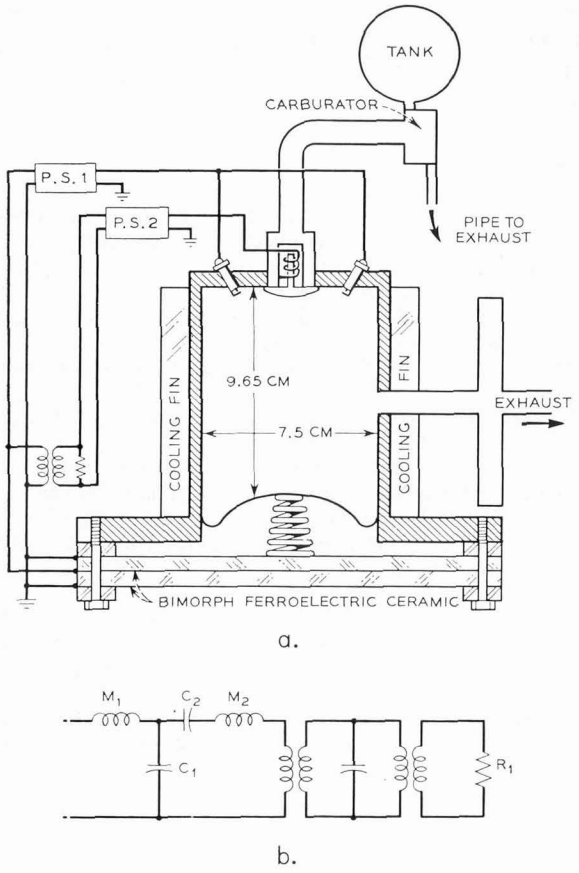

FIG. 18. — Vibration engine coupled to a ceramic flexure disk for generating power [19] (after Mason).

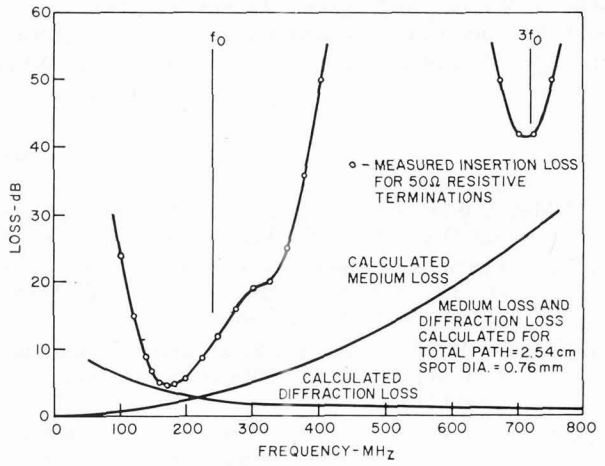

FIG. 19. — Loss versus frequency of bonded lithium niobate thickness shear transducer 10 μ thick. The graph shows calculated curves for medium loss and diffraction loss (after Warner and Meitzler [20]).

frequencies to store high bit rates and to produce light modulators and deflectors capable of rapid action. Transducers for these applications are usually single crystals of ferroelectrics such as lithium niobate, lithium tantalate or barium sodium niobate.

All these materials are ferroelectric. They can be grown from the melt by the Czochralski technique. Lithium niobate ($LiNbO_3$) has a Curie temperature of 1 210 °C and to obtain it in a single domain form it has to be cooled under an electric field of 0.2 to 5 V/cm. The material belongs to the 3 m point group. The most useful cut is an X-cut which produces a high coupling (0.68) for a shear mode with its particle velocity 41° from the Z axis. The plate can be attached to a medium such as fused silica or a crystalline medium (which will have a lower acoustic loss) by evaporating thin layers of indium on both layers and pressing them together with pressures of 1 000 to 10 000 pounds per square inch by a pneumatic press inside a vacuum chamber. After this the thickness of the transducer can be adjusted to the desired thickness by lapping or sputtering [20]. Figure 19 shows some experimental results obtained by Warner and Meitzler [20] for a fused silica medium of length 2.54 cm.

Another ferroelectric crystal of some interest is lithium tantalate ($LiTaO_3$). This has a Curie temperature of 660 °C. This does not have as high a coupling as $LiNbO_3$ but has the property that one of its cuts has a zero temperature coefficient of frequency. This is of interest in surface wave delay lines and in monolithic crystal filters.

Finally barium-sodium-niobate ($Ba_2NaNb_5O_{15}$) is a ferroelectric crystal having some interesting properties. At room temperature the crystal is orthorhombic (class mm2). The Curie Temperature is 560 °C and the crystal is tetragonal at that temperature. At 300 °C the crystal undergoes a phase transition from tetragonal to orthorhombic. It was grown principally as a non linear optic device but is useful in setting up longitudinal waves since it has a thickness coupling constant of (0.57).

All these crystals are potentially useful in the range of 100 mHz to 500 mHz and will doubtless find applications in some of the ultrasonic device applications.

6. **Evaporated thin film transducers.** — In the frequency range above 500 mHz the evaporated film technique holds the dominant position. Zinc oxide and cadmium sulphide are the materials that are most easily evaporated or sputtered. The techniques of evaporating or sputtering are rather complex and since they are described in detail [20] they will not be discussed here. The thickness can be controlled sufficiently well so that fundamental modes as high as 2 gHz have been obtained [20]. The coupling factors of these two materials are considerably less than ferroelectric single crystals i. e. ZnO $k_D = 0.24$; CdS, $k_D = 0.16$; $k_S = 0.24$, where k_D is the dilational (longitudinal coupling) and k_S the shear coupling.

The principal uses for these high frequency trans-

ducers are in delay lines for high megabit storage and for acoustic holagraphy, information storage by optical means, and other applications. While 100 megabits/s storage has been obtained experimentally [20] neither this or optical devices are used commercially at the present time.

References

[1] MASON W. P., Chap. 7. Electromechanical transducers and Wave filters D. Van Nostrand (1942).

[2] SPENCER W. J., Monolithic Filters, Physical Acoustics, vol. IX, Academic Press (1972), W. P. Mason and R. N. Thurston Editors.

[3] MASON W. P., Chap. VI. Piezoelectric crystals and their application to ultrasonics, D. Van Nostrand (1950).

[4] KIKUCHI Y., in Ultrasonic Transducers (Y. Kikuchi editor) Corona Publishing Co. Tokyo (1969).

[5] KIKUCHI Y., Ultrasonic Transducer Materials, Chap. 1 (Edited by Oskar E. Mattiat), Plenum Press New York (1971).

[6] Reference 1, 233.

[7] BUSCH G. and SCHERRER P. *Naturwissenschaften* **23** (1935) 737.

[8] MASON W. P. and MATTHIAS B., *Phys. Rev.* **88** (1952) 477.

[9] VON HIPPEL A., BRECKENRIDGE R. G., CHESLEY F. G. and TISZA L., *Ind. Eng. Chem.* **38** (1946) 1097.

[10] WUL B. and GOLDMAN I. M., *C. R. Acad. Sci. USSR* **46** (1945) 139 ; **49** (1945) 177 ; **51** (1946) 21.

[11] REMEIKA J. P., *J. Am. Chem. Soc.* **76** (1954) 940.

[12] MERZ W. J., *Phys.* **76** (1949) 1221.

[13] DEVONSHIRE A. F., Theory of Ferroelectric Crystals, *Phil. Mag. Suppl.* **3** (1954) 85.

[14] KAY H. F. and VOUSDEN P., *Phil. Mag.* **40** (1949) 1019.

[15] JAFFE B., ROTH R. S. and MARZULLO S., *J. Appl. Phys.* **25** (1954) 809.

[16] JAFFE H., *J. Am. Ceramic Soc.* **41** (1958) 494.

[17] See Ultrasonic Transducer Materials, Edited by Oskar E. Mattiat, Plenum Press (1971), Chap. II by Don Berlincourt 100-110 for effects of substitutions.

[18] Réf. 17, 87.

[19] MASON W. P., « Energy Conversion in the solid State, US Dept of Defense seminar on Advanced Energy Sources Los Angeles, Cal. Nov. (1958), 168-180 of Proceedings.

[20] These crystals, the bonding techniques and the results obtained are discussed in reference [17] (1971).